European Journal of Soil Science, August 2007, **58,** 932–944 doi: 10.1111/j.1365-2389.2007.00931.x

Surface complex structures modelled with quantum chemical calculations: carbonate, phosphate, sulphate, arsenate and arsenite

J. D. KUBICKI[a], K. D. KWON[a], K. W. PAUL[b] & D. L. SPARKS[b]
[a]*The Pennsylvania State University, Department of Geosciences and the Earth and Environmental Systems Institute, University Park, PA 16802, and* [b]*University of Delaware, Department of Plant and Soil Sciences, Newark, DE 1971,7 USA*

Summary

Hybrid molecular orbital/density functional theory (MO/DFT) calculations on molecular clusters were used to model infrared (IR) vibrational frequencies and interatomic distances obtained via extended X-ray absorption fine structure (EXAFS) spectroscopy. Molecular clusters were found to provide good agreement with experimental observations for the oxyanions carbonate, phosphate, sulphate, arsenate and arsenite. The results show a consistent tendency to form bidentate bridging surface complexes at low pH, but the protonation and hydration states play a significant role in the results obtained from calculation as various protonation states of monodentate surface complexes are also predicted to be stable as pH increases (i.e. the number of H^+ ions in the model are decreased). A method for estimating the Gibbs free energy of adsorption (ΔG_{ads}) is discussed to complement the comparisons of experimental and theoretical spectroscopic parameters. Calculated ΔG_{ads} values were consistent with the interpretations based on modelling observed spectra.

Introduction

Sorption of oxyanions is a common and important process in soils. Whether affecting the availability of nutrients or the transport of contaminants, the interaction of species such as carbonate, phosphate, sulphate, arsenate and arsenite with metal oxide and clay surfaces must be understood to predict their transport behaviour. Oxyanion surface complexes have been studied using a variety of techniques, such as Fourier transform infrared (FTIR) and EXAFS spectroscopy in order to help constrain surface complexation models. However, interpretation of the spectroscopic data is not always unambiguous. In these cases, molecular modelling can help make spectral assignments and provide valuable input to surface complexation modelling studies (Zhang *et al*., 2004; Fitts *et al*., 2005). This paper will examine principles behind modelling the oxyanion surface complexes and provide examples of how these principles can be applied to soil chemical and geochemical problems.

To begin understanding oxyanion adsorption to mineral surfaces, molecular modelling of carbonate, phosphate, sulphate, arsenate and arsenite interactions with Al and Fe hydroxide dimers was performed (Kwon & Kubicki, 2004; Bargar *et al*., 2005; Paul *et al*., 2005; Kubicki, 2005). This suite of oxyanions is not comprehensive nor is the selection of model substrates meant to simulate every adsorption reaction for these compounds in the environment. However, amorphous and crystalline Al and Fe (hydr)oxides are important reactive minerals in many soils throughout the world and metal oxides have been established as some of the most important substrates in environmental chemistry (Brown *et al*., 1999). These models were used to demonstrate how important molecular scale information can be obtained using computational chemistry and to explore how environmental factors (e.g. including solvation by H_2O) affect the accuracy of results. By obtaining results for each compound with similar methodologies, individual systems may be comparable (e.g. predictions for surface complex structures and adsorption energies).

Carbonate is a ubiquitous anion in soils and groundwaters. Carbonate complexation to metals in soil solution and on mineral surfaces is appreciable; hence understanding the surface speciation of carbonate is a prerequisite to investigating other oxyanion adsorption behaviour. Generally, carbonate will compete with other soil solution species for surface sites (Appelo *et al*., 2002; Wijnja & Schulthess, 2002; Arai *et al*., 2004). Modelling of carbonate adsorption onto haematite (α-Fe_2O_3) was performed to assess the utility of applying computational chemistry

Correspondence: J. Kubicki. E-mail: kubicki@geosc.psu.edu
Received 24 February 2007; revised version accepted 14 May 2007

calculations on molecular clusters as models of surface reactions (Bargar *et al*., 2005). In addition, the role of coadsorbed H_2O on predicted vibrational frequencies was investigated.

Phosphorus is an essential plant and animal nutrient and a component of biopolymers found in soils (Omoike *et al*., 2004). Unmanaged P (typically as phosphate) losses from watersheds are known to degrade water quality, for example in eutrophication. The transport and bioavailability of phosphate in soils is partly regulated by sorption reactions with Al and Fe (hydr)oxides. Phosphate sorption should be understood at the molecular scale in order to manage it effectively in the environment. Quantum chemical calculations were performed to help resolve controversy regarding phosphate surface complexes on Fe (hydr)oxides from IR studies (Kwon & Kubicki, 2004). Molecular modelling of six possible surface complexes was conducted to assess potential surface complexes. The calculated IR frequencies were compared to experimental IR frequency data (Persson *et al*., 1996; Arai & Sparks, 2001). In addition, reaction energies of phosphate adsorption were calculated.

Sulphur is also an essential plant and animal nutrient (sulphate is the most common form absorbed). Sulphate may become highly concentrated in soils due to geochemical cycling of metal sulphides (particularly pyrite) or to field-scale application of alum ($Al_2(SO_4)_3$) which is used to sequester phosphate in soil management practice. Recently, attenuated total reflectance (ATR) FTIR complemented by quantum chemical calculations was used to investigate sulphate adsorption on Fe (hydr)oxides and oxidized pyrite (Paul *et al*., 2005; Usher *et al*., 2005). Details of the coordination geometry and species were acquired by determining which model surface complexes best correlated with measured ATR FTIR frequencies. In this manner, the number of Fe-O-S bonds and the protonation state of sulphate were assessed.

Arsenic contamination of soil and water resources around the world has gained significant attention. Sorption of As to Al and Fe (hydr)oxides is important in the transport of As in soils and aquifers and in wastewater treatment processes. Recent studies have observed strong adsorption of As(V) onto Al and Fe (hydr)oxides (Dixit & Hering, 2003). However, As(III) was observed to adsorb less to Al (hydr)oxides than to Fe (hydr)-oxides. Quantum chemical calculations were performed for previously proposed surface complexes of As(III) and As(V) on Al and Fe (hydr)oxides. Comparison of calculated and measured vibrational frequencies for aqueous As species suggests that the molecular modelling approaches may be able to describe As bonding adequately. Interatomic distances of model surface complexes were compared to values derived from EXAFS studies (Waychunas *et al*., 1993; Fendorf *et al*., 1997; Manning *et al*., 1998; Arai *et al*., 2001; Farquhar *et al*., 2002; Sherman & Randall, 2003).

Computational chemistry and molecular modelling tools are capable of addressing complex soil chemistry research questions and advancing our understanding of nutrient management and contaminant behaviour in soils. This paper highlights some of the recent successful investigations in which computational chemistry has complemented experimental research, and ultimately afforded detailed insight into important soil chemistry issues. As the ability to model soil chemical reactions of greater complexity improves, experimentalists and modellers will be able to integrate their respective approaches more fully.

Methods

Calculations were performed using the Gaussian 03 program (Frisch *et al*., 2003). Models were built with the Cerius^2 suite of programs (Accelrys Inc., San Diego, CA, USA). Visualization of vibrational modes was performed with the Molden program (Schaftenaar & Noordik, 2000). Most computations were performed on Linux clusters run by the Graduate Education and Research Services (GEaRS) at The Pennsylvania State University (PSU) in conjunction with the Materials Simulation Center (www.msc.psu.edu) of the PSU Materials Research Institute and the Center for Environmental Kinetics Analysis (www.ceka.psu.edu). Model calculations of this size typically run efficiently on 8–16 processors and require less than 100 hours of CPU time; 512 MB of RAM/processor is generally sufficient to perform calculations of the size and basis set discussed in this paper.

Calculations were performed with a hybrid MO/DFT method. MO/DFT is a computationally efficient method for estimating electron correlation effects. The 3-parameter electron exchange functional of Becke (1993) was used in combination with the electron exchange energy derived from Hartree-Fock theory (Foresman & Frisch, 1996). The correlation functional of Lee *et al*. (1988) was used to account for electron correlation. The basis sets 6–31G(d), 6–31+G(d), and 6–311 + G(d,p) (Krishnan *et al*., 1980; McLean & Chandler, 1980; Petersson *et al*., 1988) were employed for energy minimizations, frequency calculations, and single-point energy calculations on various cluster models. The particular basis set associated with each result will be noted.

Cluster models were energy-minimized with internal redundant coordinates (Peng *et al*., 1996) and without symmetry or geometrical constraints. The use of internal redundant coordinates speeds up the process of finding potential energy minima for molecules because the derivatives of the potential energy with respect to all atomic interactions are calculated at each step. Typically, there are 3N–6 internal coordinates (where N is the number of atoms in a molecule and the 6 subtracts the rotations and translations of the molecule) required to describe atomic positions. However, using internal redundant coordinates allows the atomic positions to be adjusted into new lower energy positions more accurately than the minimum 3N–6 derivatives because all atomic interactions are accounted for simultaneously.

Default energy and structure convergence criteria in Gaussian 03 (Frisch *et al*., 2003) were used. All nuclear positions in the

models were allowed to relax to minimum potential energy positions, which is required before performing frequency calculations (i.e. the potential energy derivative for all atomic displacements must be equal to 0 in order for the harmonic approximation to be applicable). An analytical method to solve the second derivative potential energy matrix (i.e. the Hessian matrix) provided the model frequencies. Calculated frequency values were scaled by factors determined *a priori* to account for anharmonicity, basis set limitations, and the inexact determination of electron correlation (Scott & Radom, 1996; Wong, 1996). Scaling factors reduced the calculated frequencies by approximately 4%.

Correlations of observed and calculated frequencies were made by matching frequencies of vibrational modes with significant IR activity to measured frequencies. The algorithm of Yamaguchi *et al.* (1986) for calculating infrared intensities (A) analytically was used to obtain IR activities in km mol^{-1}

$$A = [1/(100\ C\ l)] \int \ln(I_o/I)\ \mathrm{d}v, \qquad (1)$$

where A is the activity (km mol^{-1}), C is the concentration (mol litre^{-1}), l is the path length (cm), I_o is the incident intensity, and I is the intensity of the transmitted radiation and v is in cm^{-1} (see Overend, 1982; Kubicki *et al.*, 1993). Although the values of the IR intensities were not quantitatively used in the current research, calculated IR intensities were used to identify important IR-active frequencies to compare with observed peaks. Vibrational mode assignments were made by visual inspection of the atomic displacements created during the frequency calculation (i.e. the eigenvectors of the Hessian matrix) using Molden (version 4.0; Schaftenaar & Noordik, 2000).

The effect of solvation on the energies of aqueous and surface species was modelled by inclusion of explicit H_2O molecules near to each solute and adsorbate, including the initial surface functional groups. Aqueous-phase Gibbs free energies were based on the integral equation formalism polarized continuum model (IEFPCM; Cancès *et al.*, 1997; Cossi *et al.*, 2002), which accounts for ion–dipole and dipole–dipole interactions not obtained with explicit solvation of H_2O molecules. This 'supermolecule' approach, where species are surrounded by a shell of H_2O and a dielectric continuum, has been shown to be an effective method for modelling the effects of water on calculated reaction energies (Keith & Frisch, 1994). A larger basis set, 6–311+G(d,p), was used for these IEFPCM calculations. The thermal correction to the Gibbs free energy from the gas-phase calculations with the B3LYP/6–31G(d) method was added to the calculated aqueous Gibbs free energy.

Molecular cluster models were used (as opposed to 3-D periodic models) because they have proven to be an efficient method for calculating vibrational frequencies and interatomic distances for surface complexes. The specific models created are attempts at balancing realism and practical computational matters. For example, metal hydroxides, oxy(hydr)oxides and oxides often hydrolyze when exposed to water, so our models include either OH or OH_2 as terminal groups around the Al^{3+} and Fe^{3+} cations. Many interpretations of adsorption data suggest that bidentate bridging complexes are common for oxyanions; hence we included two metal-oxide octahedra as the basis of our surface. These octahedra are linked by OH groups because similar structures may exist on surfaces of minerals such as goethite (α-FeOOH) and diaspore (α-AlOOH). Although limited in their representation of some oxides, such as haematite (α-Fe_2O_3), this model was chosen as a compromise between the metal hydroxides and oxides. Good reproduction of observed vibrational frequencies for surface complexes on a variety of Al and Fe minerals has justified this simplification, but more specific models can be created to mimic particular mineral surfaces (Kubicki & Apitz, 1998).

One weakness of the molecular cluster model for surfaces is that crystal structure constraints are not imposed upon the surface functional groups and surface complexes. Periodic models may more realistically represent surfaces, but the calculated vibrational frequencies and interatomic distances (as compared with IR/Raman and EXAFS) have not yet proven to be superior compared with molecular cluster models (research into this topic is currently underway, see Paul *et al.*, 2007, in this issue). Furthermore, current work on calculated Gibbs free energies of adsorption suggests that the molecular cluster approach can predict thermodynamics reasonably accurately. Hence, 3-D periodic models have utility for examining longer-range effects and defect structures; but, for our purposes here, the significant increase in computational time required is not justified.

Results

Carbonate adsorption on haematite

Haematite is common in soils and aquifers and is a strong adsorbent of oxyanions due to its positive surface charge at circumneutral pH. Although other Fe oxy(hydr)oxides are more common in soils, similar adsorption mechanisms may be operative on these surfaces when examining inner-sphere complexation. Hence, haematite has been used as a model substrate for examining adsorption of oxyanions to Fe oxy(hydr)oxide surfaces.

At least 10 possible configurations exist for CO_3^{2-} adsorption onto Fe oxy(hydr)oxides (Bargar *et al.*, 2005). Combinations among the configurations of monodentate versus bidentate, carbonate versus bicarbonate and inner- versus outer-sphere adsorption contributed to the ambiguity of interpreting earlier IR spectra (e.g. Su & Suarez, 1997; Wijnja & Schulthess, 2001). Moreover, the possibility that speciation could change with pH and that several surface complexes could coexist under any given set of conditions further complicated the situation. Consequently, Bargar *et al.* (2005) measured ATR FTIR spectra of carbonate adsorbed onto haematite as a function of pH and with replacement of H_2O by D_2O. Systematic

data analysis of the spectra demonstrated a potential inner-sphere complex with C-O_s and C-O_{as} modes (symmetric (s) and asymmetric (as) C-O bond stretching which are the most intense IR modes of carbonate vibrations) at 1320 and 1530 cm^{-1}, respectively. In addition, a potential outer-sphere complex with C-O_s and C-O_{as} vibrations at 1360 and 1470 cm^{-1}, respectively, was also observed.

MO/DFT calculations (B3LYP/6–31G(d)) were performed on several variations of carbonate and bicarbonate adsorption, but none of the model calculations provided predicted frequencies within computational error (typically 20 cm^{-1}) of experimental frequencies. The bidentate bridging configuration (Figure 1), considered the most likely surface complex, resulted in frequencies in error by *c*. 200 cm^{-1} with splitting between the C-O_s and C-O_{as} modes ($\Delta\nu$) of 542 cm^{-1} (compared to the observed $\Delta\nu$ of 210 cm^{-1}; Bargar *et al*., 2005). Bidentate bridging HCO_3^- predicted a $\Delta\nu$ of 200 cm^{-1}; however, values of the C-O_s and C-O_{as} frequencies were in error by *c*. 100 cm^{-1}.

Previous results had shown much better agreement with observed frequencies (Kubicki *et al*., 1997). Bargar *et al*. (2005) hypothesized that the discrepancy may be due to the models selected rather than the computational methodology. Earlier papers on similar systems had shown that drying samples with adsorbed oxyanions could significantly change the observed frequencies of the oxyanion surface complex (e.g. Hug, 1997; Myneni *et al*., 1998). Because the samples in Bargar *et al*. (2005) were not dried, two H_2O molecules were added to form hydrogen bonds with the carbonate surface complexes (Figure 1b), to mimic the *in situ* hydrated experiment. The effects were dramatic. The aforementioned bidentate bridging carbonate frequencies (C-O_s and C-O_{as}) changed from 1166 and 1708 cm^{-1} to 1329 and 1524 cm^{-1}, respectively, within computational error of the observed 1320 and 1530 cm^{-1} bands. The calculated $\Delta\nu$ value decreased from 542 to 195 cm^{-1}, much closer to the observed splitting of 210 cm^{-1}. Addition of four more H_2O molecules changed the calculated frequencies by 10 cm^{-1} or less, indicating that inclusion of H-bonding was a key to obtaining accurate model frequencies. Furthermore, this indicates that at least a monolayer of water exists on mineral surfaces with adsorbed oxyanions even after air drying, due to strong H-bonding.

Solvating an outer-sphere carbonate anion near the Fe (hydr)oxide cluster with 10 H_2O molecules also resulted in good agreement between observed (1360 and 1470 cm^{-1}) and model C-O_s and C-O_{as} frequencies (1346 and 1460 cm^{-1}). Bargar *et al*. (2005) concluded that relatively simple molecular cluster models were capable of predicting the vibrational modes of mineral surface complexes. Furthermore, a moderate level of theory was able to provide accurate results within 10–20 cm^{-1} of the C-O_s and C-O_{as} frequencies and $\Delta\nu$.

Phosphate adsorption on goethite

Based on the work of Persson *et al*. (1996) and Arai & Sparks (2001), six possible species of orthophosphate (Figure 2) were

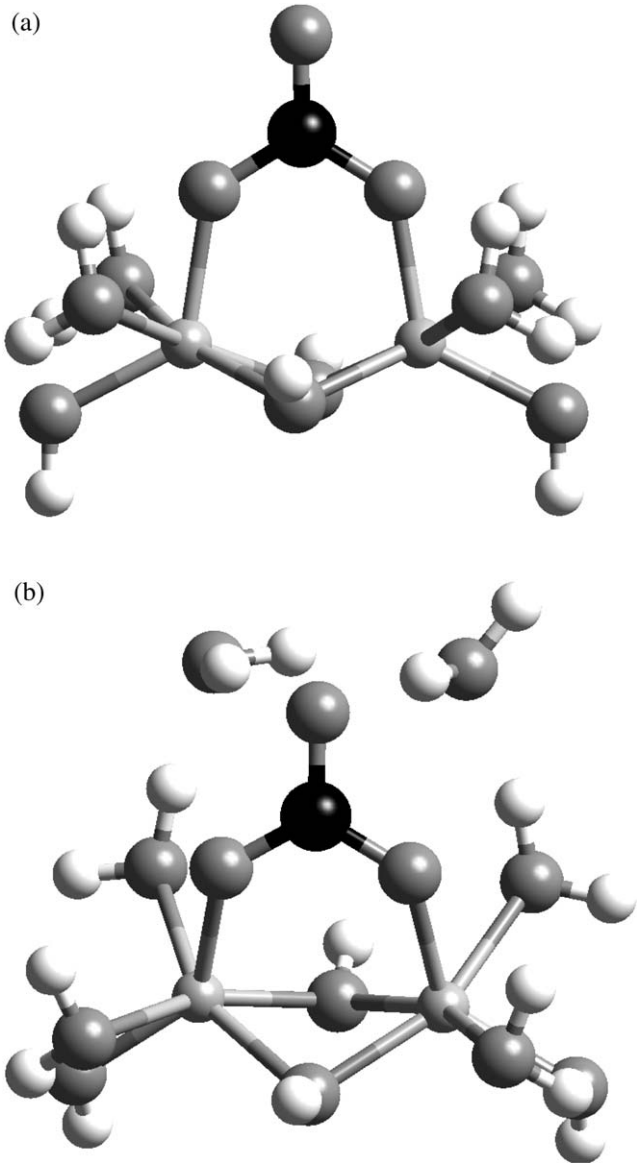

Figure 1 Carbonate on $Fe_2(OH)_4(OH_2)_4$ (a) without solvation and (b) with solvation by two H_2O molecules. H = white, C = black, O = dark grey, and Fe = light grey. Graphics created with Cerius^2 (Accelrys Inc., San Diego, CA, USA).

thought to form on the surface of goethite (α-FeOOH) and 2-line ferrihydrite, respectively. These results highlight the point that similar surface complexes of a given oxyanion can form on a variety of mineral surfaces. IR interpretations depended on the use of symmetry arguments to predict the number of bands observed for surface phosphate complexes. Hence, it was difficult to distinguish among species that varied in the number of P-O-H and P-O-Fe bonds. As in the case of carbonate adsorption, protonation states could also change as a function of pH (Persson *et al*., 1996). Quantum chemical calculations (B3LYP/6–31G(d)) were performed on the six possible species to determine which model complex produced

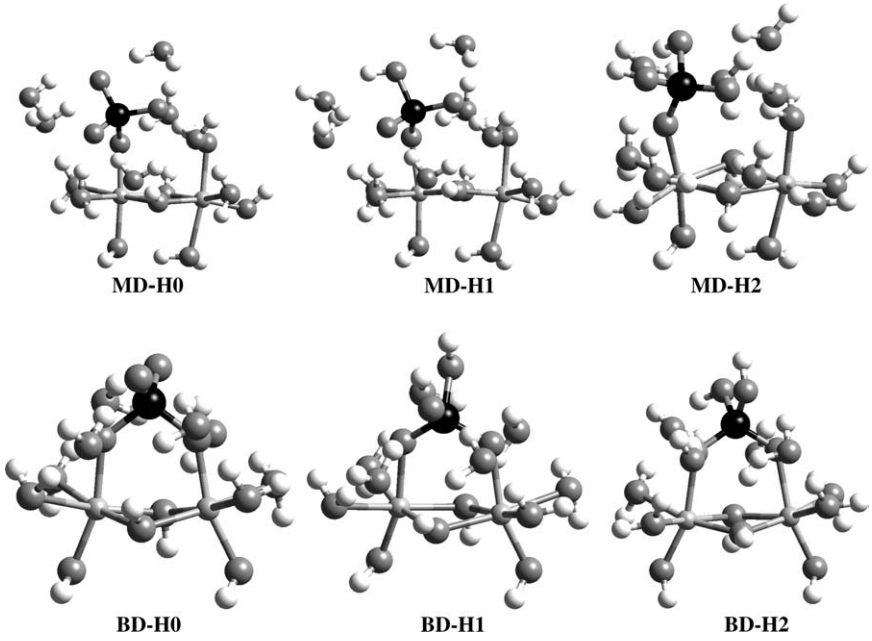

Figure 2 Possible phosphate species for adsorption onto Fe oxy(hydr)oxides. MD, monodentate; BD, bidentate; H0, H1 and H2, number of H^+ bonded to the phosphate. H = white, P = black, O = dark grey, and Fe = light grey. Graphics created with Cerius^2 (Accelrys Inc.).

vibrational frequencies in best agreement with observation (Kwon & Kubicki, 2004).

Phosphate surface complexes on goethite have four to six observed IR modes. Deconvolution of these spectra to obtain vibrational frequencies allows direct correlations to be made between the experimental and calculated values. Correlation of multiple peaks makes it possible to assign surface complexes to observed spectra reliably and with better resolution among similar structures. Figure 3 shows the calculated versus experimental correlations for acidic, neutral and basic pH conditions. Under acidic and basic conditions, the diprotonated bidentate (BD-H2) and unprotonated monodentate (MD-H0) surface complexes, respectively, preferably formed. The BD-H2 correlation had a slope = 1.00, R^2 = 0.99, and RMS error = 15 cm^{-1}, significantly closer to the ideal values of 1, 1, and 0 cm^{-1} than the other models (Kwon & Kubicki, 2004).

For spectra collected at pH 7.5 (Arai & Sparks, 2001) and 7.9 (Persson *et al*., 1996), the distinction between surface complexes was not as obvious. Two surface complexes, the deprotonated bidentate (BD-H0) and the monoprotonated monodentate (MD-H1), resulted in accurate correlations with the spectra presented in Arai & Sparks (2001) and Persson *et al*. (1996), respectively. The measured spectra were different because the experimental techniques and synthetic minerals were not identical; hence it was impossible to assign one model that accurately reproduced both data sets.

Estimates of the adsorption energy of each complex were calculated to help resolve this issue. Assuming a ligand exchange reaction involving surface water,

$$\text{Surface} + \text{Aqueous species} \rightarrow \text{Surface complex} + \text{Released } H_2O,$$

energies were calculated using B3LYP/6–311+G(d,p) single point calculations on B3LYP/6–31G(d) energy minimized structures (i.e. only the potential energy is calculated with the larger basis set and no further relaxation of the atoms is performed). An estimate of long-range solvation energy based on the IEFPCM (Cancès *et al*., 1997; Cossi *et al*., 2002) was included. Adsorption energies calculated in this manner are not expected to give highly accurate absolute energies with respect to experiment. The assumption was made that error cancellation would allow the *relative* ΔG-values to be used to predict which species would be more thermodynamically favourable. In all cases, whichever starting surface model and aqueous protonation state of orthophosphate were used, the MD-H1 was predicted to be more thermodynamically favourable than the BD-H0 model. For example, the pKa_2 of H_3PO_4 is 7.2, so both $H_2PO_4^-$ and HPO_4^{2-} were used as aqueous species. The surface charge of goethite is slightly positive at pH 7.5–7.9 (Parks, 1965) leading to the use of surface models with +1 and neutral initial charge. The ΔG-values calculated for the most likely adsorption reaction (i.e. +1 surface charge with HPO_4^{2-}) were –34 kJ mol^{-1} for the BD-H0 surface complex and –61 kJ mol^{-1} for the MD-H1 configuration. The difference of –27 kJ mol^{-1} was expected to be significant compared to the relative computational error, so the latter complex was more thermodynamically favoured. This configuration also gave the best fit (slope = 0.98, R^2 = 1.00 and RMS error = 4 cm^{-1}) to the frequencies presented in Persson *et al*. (1996). The spectra in Persson *et al*. (1996) were better resolved than those in Arai & Sparks (2001); however, Kwon & Kubicki (2004) were able to convolute the model frequencies to reasonably represent the Arai & Sparks (2001) spectra based on the same calculated frequencies that matched the Persson *et al*. (1996) data.

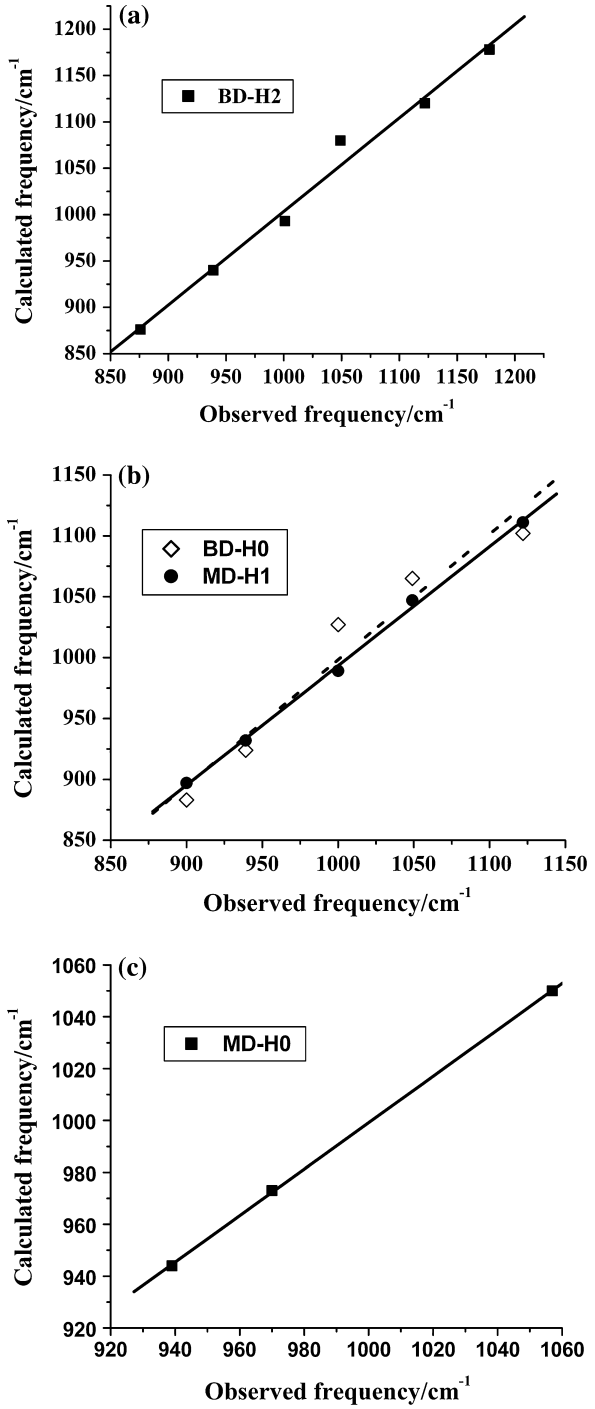

Figure 3 Frequency correlations of observed and modelled modes of orthophosphate complexes on goethite (experimental values from Persson *et al*., 1996). (a) pH 4.2, (b) pH 7.9, and (c) pH 12.8.

Organophosphate and bacterial adsorption

With orthophosphate adsorption as a test case, Omoike *et al*. (2004) used similar methods to interpret the molecular mechanism of bacterial exopolymer adsorption onto goethite (α-FeOOH). Extracellular polymeric substances (EPS) were extracted from *Bacillus subtilis* and *Pseudomonas aeruginosa* and adsorbed onto an ATR FTIR cell coated with goethite particles. IR spectra of adsorbed EPS showed enhancement over the aqueous spectrum for bands in the 900–1200 cm^{-1} region commonly associated with phosphoryl vibrations. A model organophosphate, $PO_2(C_5O_3H_9)_2$, was bonded to an Fe hydroxide cluster in monodentate and bridging bidentate configurations. This compound was used because it mimics the phosphoryl groups in nucleic acids by binding two sugars to the phosphate moiety. The bases normally linked to these sugars were eliminated because they are located within the chain of nucleic acids and unlikely to bind to the Fe (hydr)oxide surfaces.

The monodentate configuration gave the better correlation to the observed frequencies (slope = 1.05, intercept = −48 cm^{-1}, R^2 = 0.98, and RMS error = 11 cm^{-1}) compared to the bidentate configuration (slope = 1.06, intercept = −63 cm^{-1}, R^2 = 0.93, and RMS error = 20 cm^{-1}). In addition, only the monodentate configuration predicted a vibrational frequency (near 1175 cm^{-1}) that was in the region of an observed band at 1150 cm^{-1}. This is a vibrational mode associated with P=O double bonds, so it is only expected in the monodentate configuration. Estimation of adsorption energies resulted in the monodentate configuration being more thermodynamically favourable by –20 kJ mol^{-1}, consistent with the interpretation of the surface complex based on the frequency correlations. This study demonstrated that phosphorylated biopolymers, either nucleic acids or phospholipids, are a key to bacterial adhesion mechanisms onto goethite. Judiciously chosen model systems allow bonding of biopolymers to mineral surfaces to be modelled with relatively small molecular clusters.

Sulphate adsorption onto Fe (hydr)oxides

Paul *et al*. (2005) examined the effect of drying on sulphate speciation and coordination on Fe (hydr)oxides. Previously, it was proposed that dehydration of Fe (hydr)oxides potentially cause a coordination and/or speciation change of adsorbed sulphate (Hug, 1997). Measurements of dried sulphate-treated haematite at pH 3.6 showed an IR band at *c*. 1200 cm^{-1}, the intensity of which increased upon further drying (this band was not present for hydrated samples). The same band also appeared when haematite was in contact with aqueous sulphate acidified below pH 2, leading to speculation that the speciation of sulphate was affected (Hug, 1997). Hence, there was clearly a connection between the hydration state and mineral surface pH that significantly affected the speciation of adsorbed sulphate.

Coupling MO/DFT calculations with ATR FTIR spectroscopy, Paul *et al*. (2005) showed that under hydrated conditions inner-sphere sulphate adsorption occurs by either monodentate or bidentate bridging mechanisms (Figure 4), possibly dependent upon mineral surface loading. Upon drying of the mineral surface a fraction of sulphate protonates to form

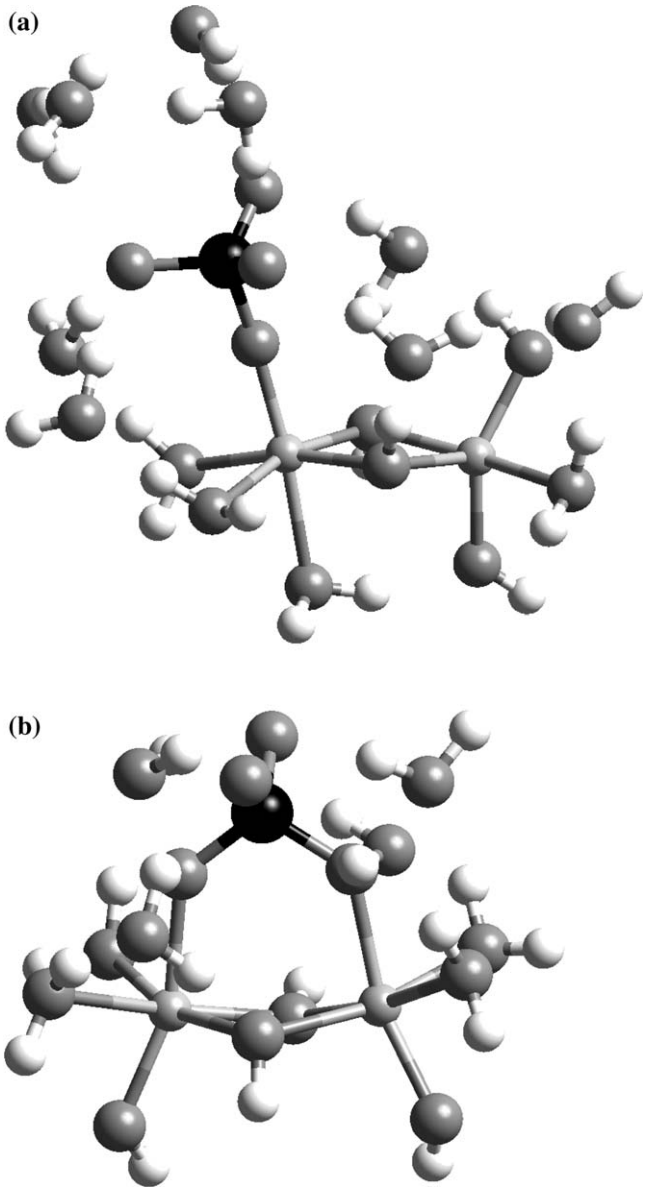

Figure 4 Inner-sphere sulphate with Fe hydroxide model surface in (a) monodentate and (b) bidentate bridging configuration. H = white, S = black, O = dark grey, and Fe = light grey. Graphics created with Cerius[2] (Accelrys Inc.).

bisulphate. Sulphate protonation and deprotonation behaviour is controlled by the hydration environment of the OH group on bisulphate. These results were important because soils naturally alternate between wet and dry conditions and a paucity of research has been conducted on this topic, though it may be quite significant for soil acidity.

Sulphate formed on pyrite during oxidation

In addition to modelling surface complexes and adsorption energies, computational chemistry is useful for modelling reaction mechanisms (see Felipe *et al*., 2001, and references therein). MO/DFT calculations (Paul *et al*., 2005; B3LYP/6–31+G(d)) were combined with experimental studies in Usher *et al*. (2005) to examine the oxidation of pyrite exposed to gaseous H_2O and O_2. ATR FTIR spectroscopy was used to monitor structural changes on the surface as oxidation occurred. The source of sulphate and bisulphate O atoms was tracked by isotopically labelling the H_2O and O_2 with ^{18}O, and it was found that both reactants could contribute to (bi)sulphate formation. MO/DFT calculations helped to interpret the ATR FTIR spectra and identify surface complexes. Subsequent work could then focus on modelling the oxidation of FeS_2 and formation of sulphate (e.g. Rosso *et al*., 1999; Becker *et al*., 2001).

Frequencies were calculated for sulphate and bisulphate complexes bonded to Fe hydroxide clusters to mimic the oxidized surface of pyrite, because Fe(II) is oxidized to Fe(III) simultaneously with oxidation of S(-I) to S(VI). The presence of two complexes explains the observed frequencies: a monodentate and a bidentate bridging bisulphate (Table 1). Examination of Table 1 shows that one complex cannot fit the observed frequencies at either low or high H_2O/O_2 ratio. However, if both the bidentate and monodentate bisulphate complexes were present, then a good match could be found for each observed frequency. The sulphate complexes resulted in predicted frequencies that were generally too low compared to experiment, and no frequencies significantly above 1100 cm^{-1} were calculated for sulphate configurations (Table 1), militating against the possibility of a sulphate surface complex.

Table 1 Observed (Usher *et al*., 2005) and calculated frequencies of sulphate and bisulphate complexes bonded to an Fe(III)-(hydr)oxide cluster. (Note that the monodentate calculated frequencies have been updated from Usher *et al*. (2005) (see Paul *et al*., 2005) because these particular model surface complexes were structurally improved and the frequencies recalculated)

Observed (cm^{-1})		Calculated (cm^{-1})			
High H_2O/O_2	Low H_2O/O_2	Bidentate Bisulphate	Monodentate Bisulphate	Bidentate Sulphate	Monodentate Sulphate
				901	906
	990	973	972	950	967
1065	1065	1076	1062	992	1003
				1029	
1108	1107			1099	1095
1145	1125		1129		
1165	1160		1175		
1190	1185	1188			
High $H^2\,^{18}O/O_2$					
				938	834
		923	928	978	944
1000			1034	1005	981
1065		1052		1066	1067
1085		1077			
1124			1100		
1158		1170	1159		

Usher *et al*. (2005) also used $H_2{}^{18}O$ and $^{18}O_2$ in their experiments; thus, it was possible to replace the ^{16}O in the sulphate group with ^{18}O in the frequency calculations and compare with observed results. Vibrational mode energies are sensitive to isotopic variations (i.e. the reduced mass of the vibration), so comparing measured and calculated $^{16}O/^{18}O$ frequency shifts could potentially help identify the surface complexes. Comparisons of the observed ^{18}O-substituted vibrational frequencies with the frequencies calculated with ^{18}O in the sulphate again favoured the bisulphate complexes over the sulphate species (Table 1). Identification of these intermediate species was an important step in the process of modelling pyrite oxidation because it constrains the reaction pathway at a point between the reactants and products. Without such constraints along various pathways, many alternative paths exist and modelling efforts will be wasted examining unrealistic routes of reaction.

Arsenate and arsenite adsorption onto Al and Fe hydroxides

As(V) adsorbs in similar amounts to amorphous $Al(OH)_3$ and $Fe(OH)_3$ but As(III) adsorbs more strongly to amorphous $Fe(OH)_3$ than to $Al(OH)_3$. The methods employed above were applied to the As–$Fe(OH)_3$ and As–$Al(OH)_3$ systems to help explain this observation. Although calculations of aqueous As species (H_3AsO_3, $H_2AsO_3^-$, $H_2AsO_4^-$, and $HAsO_4^{2-}$) surrounded by eight H_2O molecules reproduced observed vibrational frequencies (IR and Raman) with reasonable accuracy (data not shown), the IR and Raman spectra of adsorbed As species showed only one or two broad peaks between 630 and 850 cm^{-1} (Goldberg & Johnston, 2001). Most of the surface complexes predicted frequencies in this region, so interpretation of the surface structures based on vibrational frequencies did not seem feasible. Computing the ΔG of adsorption could be used; but, as mentioned above, this method may not be highly accurate, with potential relative errors of more than $\pm$ 10 kJ mol^{-1}. Hence, it was possible that several model structures could be possible, based solely on calculated adsorption energies. Another primary data set was necessary to reduce the number of models that could potentially be consistent with the experiment.

Fortunately, EXAFS studies have been carried out for As adsorbed to Fe and Al oxy(hydr)oxides (Waychunas *et al*., 1993; Fendorf *et al*., 1997; Manning *et al*., 1998; Arai *et al*., 2001; Farquhar *et al*., 2002; Sherman & Randall, 2003). Interpretation of EXAFS data can be difficult, but the results commonly provide coordination numbers and interatomic distances for adsorbed species. Energy minimizations using MO/DFT provide molecular structures as output and calculating accurate structures requires less effort than calculation of adsorption energies or vibrational frequencies. The main concern for comparing the model calculations would be whether the molecular clusters could accurately represent surface complex interatomic distances. Based on the ability to reproduce observed vibrational frequencies, it was assumed that the molecular clusters would be useful to compare with EXAFS data.

The difference in As(III) adsorption to $Fe(OH)_3$ and $Al(OH)_3$ was perplexing because the primary adsorption product was thought to be the bidentate bridging configuration for both species (Figure 5). To test this interpretation, a series of monodentate and bidentate bridging surface complexes were energy-minimized (B3LYP/6–31G(d); Kubicki, 2005). In general, the results were consistent with the previous interpretation of Waychunas *et al*. (1993) and Arai *et al*. (2001), namely that the bridging bidentate configurations were favoured. For example, the observed As-O and As-Fe distances for As(III) adsorbed onto Fe oxy(hydr)oxides were 1.78 and 3.38 Å, respectively (Waychunas *et al*., 1993; Farquhar *et al*., 2002). The model surface complex $Fe_2(OH)_4(OH_2)_4AsO_3{\cdot}(H_2O)_4$ (Figure 5a) resulted in distances of 1.76 and 1.80 Å for As-O and 3.28 Å for As-Fe, consistent with the experiment.

One question that remained was the protonation state of adsorbed As(III) and As(V) on the mineral surfaces. For As(III), this question was resolved by calculating the structure of the (Al or $Fe)_2(OH)_4(OH_2)_4HAsO_3$ complexes. The As-OH bond length was predicted to be 1.93 and 1.89 Å for the Al and Fe models, respectively. This distance was significantly longer than the observed value of 1.78 Å, so the protonated As(III) bidentate bridging model was rejected in favour of (Al or $Fe)_2(OH)_4(OH_2)_4AsO_3$.

For As(V), Sherman & Randall (2003) found three As-O distances at approximately 1.71 Å and a fourth at 1.62 Å. Of the models tested, the best fit was obtained for the $Fe_2(OH)_4(OH_2)_4$-$HAsO_4$ cluster where the As = O distance was equal to 1.63 Å, the As-OH bond distance was equal to 1.83 Å, and the As-O (Fe) bond distances were equal to 1.72 Å. With H_2O added (i.e. $Fe_2(OH)_4(OH_2)_4HAsO_4{\cdot}(H_2O)_4$; Figure 5c), these values changed to As=O 1.66, As-OH 1.77, and As-O(Fe) 1.71 Å. Protonating the AsO_4 group and forming the As = O appears to be the only method for creating an As-O distance near 1.62 Å.

To model accurately As surface complexes, the protonation state and explicit hydration were critical. The protonation state of As(III) and As(V) species had a strong influence on the calculated bond lengths. Thus, when one is using experimental interatomic distances to determine surface complex configurations, modelling the correct protonation state is important. Protonation and hydration are interrelated because unprotonated, highly charged oxyanions promote H^+ transfers from the model surface to themselves if they are not H-bonded to H_2O molecules. H-bonding directly influences the calculated oxyanion bond lengths, but to a lesser degree. When modelling relative thermodynamic stabilities of surface complexes, the protonation state of the oxyanion influences the calculated energies. Larger charge differences between the negative adsorbate and positive model surface lead to dramatic increases in calculated ΔG of adsorption (see Kwon & Kubicki,

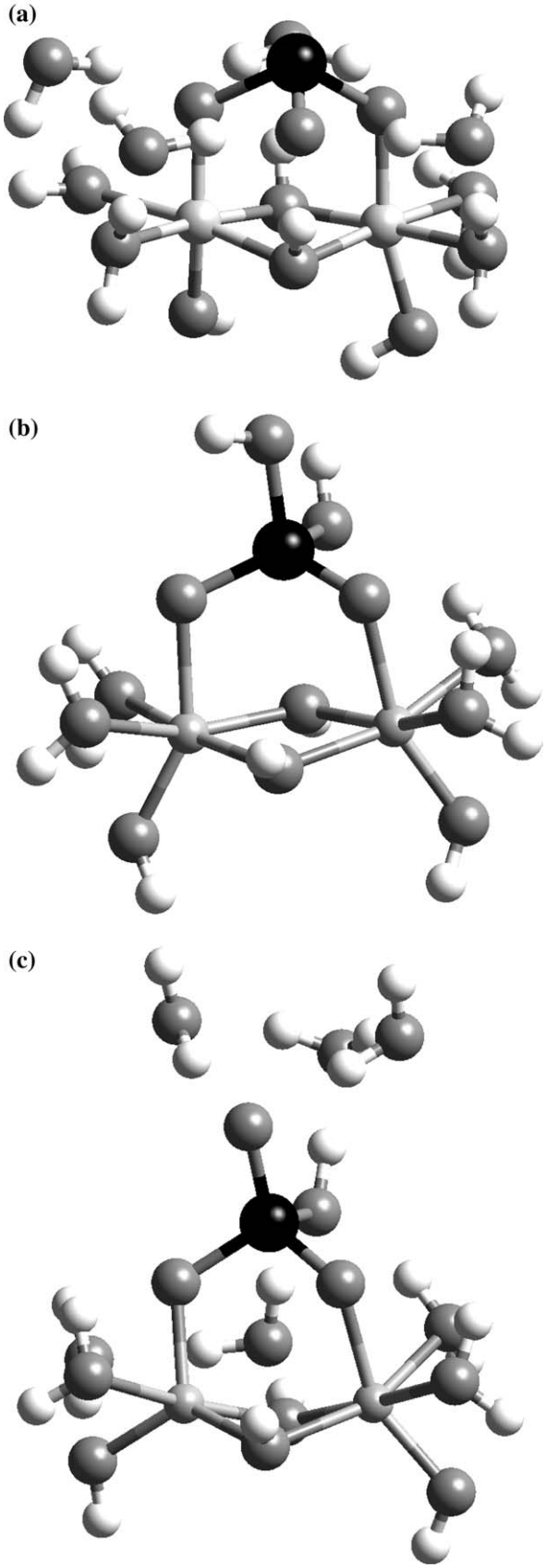

2004, for the effect of changing charge from 0 to +2 for model Fe (hydr)oxides.).

Although other configurations of As surface complexes on Fe and Al (hydr)oxides may be possible (Waychunas *et al*., 2006), the energetic analysis here focused on the bidentate bridging configurations of As(III) and As(V). This complex is likely to be the dominant configuration under most pH conditions. Furthermore, comparing model ΔG_{ads} values was simplified by examining similar configurations in various combinations of As(III), As(V), model $Al(OH)_3$ and $Fe(OH)_3$. For As(V) adsorption under neutral pH conditions, the following two reactions are most likely because pK_{a2} of arsenious acid is 7 (i.e. $[H_2AsO_4^-] = [HAsO_4^{2-}]$ at pH 7):

$$H_2AsO_4^- \cdot (H_2O)_8 + M_2(OH)_5(OH_2)_5^+ \cdot (H_2O)_4 \rightarrow M_2(OH)_4(OH_2)_4HAsO_4 \cdot (H_2O)_4 + 10H_2O$$

and

$$HAsO_4^{2-} \cdot (H_2O)_8 + M_2(OH)_5(OH_2)_5^+ \cdot (H_2O)_4 \rightarrow M_2(OH)_4(OH_2)_4HAsO_4 \cdot (H_2O)_4 + [OH^- \cdot (H_2O)_4] + 5H_2O,$$

where M = Al(III) or Fe(III) and the model surface has a positive charge. The calculated ΔG_{ads} values for these two reactions were –94 and –140 kJ mol^{-1} for the first reaction on Al and Fe (hydr)oxides, respectively, and –151 and –197 kJ mol^{-1} for the second reaction on Al and Fe (hydr)oxides, respectively. Thus, As(V) adsorption was predicted to be more thermodynamically favoured onto Fe (hydr)oxide than Al (hydr)oxide, but the ΔG_{ads} are both so favourable for As(V) that the adsorption sites may be saturated with respect to As(V) for both substrates.

For As(III) adsorption, a probable reaction at pH 7 is

$$H_3AsO_3 \cdot (H_2O)_8 + M_2(OH)_5(OH_2)_5^+ \cdot (H_2O)_4 \rightarrow M_2(OH)_4(OH_2)_4AsO_3^- \cdot (H_2O)_4 + 2[H_3O^+ \cdot (H_2O)_4].$$

H_3AsO_3 should dominate the aqueous speciation because pK_{a1} for arsenious acid is 9.2. The model ΔG adsorption was +57 and +14 kJ mol^{-1} for the Al and Fe hydroxides, respectively (Kubicki, 2005). Neither is thermodynamically favoured but the Fe hydroxide is calculated to be significantly less positive than the Al hydroxide reaction. The +14 kJ mol^{-1} value is close to zero within our computational error.

Figure 5 (a) As(III) with H_2O on $Me_2(OH)_4(OH_2)_4$, (b) As(V) on $Me_2(OH)_4(OH_2)_4$ diprotonated without H_2O, and (c) As(V) monoprotonated with H_2O. H = white, As = black, O = dark grey, and Al, Fe = light grey. Graphics created with Cerius[2] (Accelrys Inc.).

Another possible reaction involves the minor species (at pH 7) $H_2AsO_3^-$:

$$H_2AsO_3^- \cdot (H_2O)_8 + M_2(OH)_5(OH_2)_5^+ \cdot (E_2O)_4 \rightarrow M_2(OH)_4(OH_2)_4AsO_3^- \cdot (H_2O)_4 + H_3O^+ \cdot (H_2O)_4 + 5H_2O.$$

ΔG_{ads} calculated for these species were +37 and –7 kJ mol^{-1} on Al and Fe hydroxides, respectively. The calculated ΔG_{ads} value for As(III) adsorption onto Al hydroxide is positive and slightly negative for Fe hydroxide, which is qualitatively consistent with the observation of greater As(III) adsorption to Fe (hydr)oxide than Al (hydr)oxide (Hering *et al.*, 1997; Dixit & Hering, 2003). Thus, the minor $H_2AsO_3^-$ aqueous species will preferentially adsorb onto Fe hydroxides and the aqueous equilibrium will adjust by deprotonating more H_3AsO_3 in solution. All likely model reactions involving the protonated bidentate As(III) surface complex, $M_2(OH)_4(OH_2)_4HAsO_3^- \cdot (H_2O)_4$, resulted in positive calculated ΔG_{ads} values. Consequently, the $Fe_2(OH)_4(OH_2)_4AsO_3^- \cdot (H_2O)_4$ species (Figure 5a) appeared to be the most likely on Fe hydroxides, based on Gibbs free energy calculations. This conclusion was the same as that based on comparing interatomic distances from EXAFS with the molecular models. The fact that both approaches point toward the same surface complex helps validate this approach and strengthen the conclusions drawn from it.

Comparison of model adsorption energies

Although calculating absolute reaction Gibbs free energies for mineral–water interface reactions is challenging, it can be instructive to compare the relative model ΔG_{ads} for this series of oxyanions (see Radu *et al.*, 2005 for examples). Because these calculations can be conducted self-consistently, the relative adsorption energies provide insight into the thermodynamic favourability of adsorption in multicomponent systems. This is especially true for the species of interest here (carbonate, phosphate, sulphate, arsenate and arsenite) because these compounds may adsorb at similar sites on Fe and Al (hydr) oxide surfaces.

The aqueous species HCO_3^-, $H_2PO_4^-$, HPO_4^-, SO_4^{2-}, $H_2AsO_4^-$, $HAsO_4^-$, H_3AsO_3 and $H_2AsO_3^-$ were chosen because these should be present in finite quantities at pH 7 according to their pK_a values (Faure, 1998). Other species could be included to examine model predictions at other pH values, but, for the sake of simplicity, only these species will be discussed here. The product surface complexes were selected based on comparisons to experimental data as discussed above. To further simplify the comparison, model surface sites with a +1 charge were included as potential reactants. Restricting the analysis to the +1 model surface helped limit the role of electrostatics in the calculated adsorption energies. Aqueous species of identical charge could not be used in each case, however, because we were constrained by the species that actually exist in solution. Hence, electrostatics still play a role in the calculated adsorption energies, but the nature of our calculations allows for implicit inclusion of this factor in our model results. Neutral adsorption sites can also be important, but the adsorption energies were consistently larger for the +1 model surface, so these sites should dominate adsorption in real systems when the concentrations of potential adsorbates are small.

The following ΔG_{ads} were modelled at the B3LYP/6–311+G(d,p)//B3LYP/6–31G(d) level of theory with the Gibbs free energy from the IEFPCM solvation model (Cancès *et al.*, 1997) corrected by the gas-phase thermal correction to the Gibbs free energy with the B3LYP/6–31G(d) method:

$$HCO_3^- \cdot (H_2O)_6 + Fe_2(OH)_5(OH_2)_5^+ \cdot (H_2O)_4 \rightarrow Fe_2(OH)_4(OH_2)_4CO_3 \cdot (H_2O)_6 + 1.2[(H_2O)_5] = -51 \text{ kJ mol}^{-1}$$

$$H_2PO_4^- \cdot (H_2O)_8 + Fe_2(OH)_5(OH_2)_5^+ \cdot (H_2O)_4 \rightarrow Fe_2(OH)_4(OH_2)_4H_2PO_4^+ \cdot (H_2O)_4 + [OH^- \cdot (H_2O)_4] + 5H_2O = +75 \text{ kJ mol}^{-1}$$

$$H_2PO_4^- \cdot (H_2O)_8 + Fe_2(OH)_5(OH_2)_5^+ \cdot (H_2O)_4 \rightarrow Fe_2(OH)_4(OH_2)_4HPO_4^+ \cdot (H_2O)_4 + 10H_2O = -128 \text{ kJ mol}^{-1}$$

$$H_2PO_4^- \cdot (H_2O)_8 + [Fe_2(OH)_5(OH_2)_5^+ \cdot (H_2O)_4] \rightarrow Fe_2(OH)_4(OH_2)_5HPO_4 \cdot (H_2O)_6 + 1.4[(H_2O)_5] = -88 \text{ kJ mol}^{-1}$$

$$H_2PO_4^{2-} \cdot (H_2O)_8 + [Fe_2(OH)_5(OH_2)_5^+ \cdot (H_2O)_4] \rightarrow Fe_2(OH)_4(OH_2)_5HPO_4 \cdot (H_2O)_6 + [OH^- \cdot (H_2O)_4] + 0.4[(H_2O)_5] = -76 \text{ kJ mol}^{-1}$$

$$SO_4^{2-} \cdot (H_2O)_9 + Fe_2(OH)_5(OH_2)_5^+ \cdot (H_2O)_4 \rightarrow Fe_2(OH)_4(OH_2)_4SO_4 \cdot (H_2O)_4 + [OH^- \cdot (H_2O)_4] + 1.2[(H_2O)_5] = -66 \text{ kJ mol}^{-1}$$

$$H_2AsO_4^- \cdot (H_2O)_8 + Fe_2(OH)_5(OH_2)_5^+ \cdot (H_2O)_4 \rightarrow Fe_2(OH)_4(OH_2)_4HAsO_4 \cdot (H_2O)_4 + 10H_2O = -140 \text{ kJ mol}^{-1}$$

$$HAsO_4^{2-} \cdot (H_2O)_8 + Fe_2(OH)_5(OH_2)_5^+ \cdot (H_2O)_4 \rightarrow Fe_2(OH)_4(OH_2)_4HAsO_4 \cdot (H_2O)_4 + [OH^- \cdot (H_2O)_4] + 5H_2O = -197 \text{ kJ mol}^{-1}$$

$$H_3AsO_3{\cdot}(H_2O)_8 + Fe_2(OH)_5(OH_2)_5^+{\cdot}(H_2O)_4 \rightarrow Fe_2(OH)_4(OH_2)_4AsO_3^-{\cdot}(H_2O)_4 + 2[H_3O^+{\cdot}(H_2O)_4] = +14\ \text{kJ mol}^{-1}$$

$$H_2AsO_3^-{\cdot}(H_2O)_8 + Fe_2(OH)_5(OH_2)_5^+{\cdot}(H_2O)_4 \rightarrow Fe_2(OH)_4(OH_2)_4AsO_3^-{\cdot}(H_2O)_4 + H_3O^+{\cdot}(H_2O)_4 + 5H_2O = -7\ \text{kJ mol}^{-1}$$

From the above model adsorption energies, a few observations can be made. First, the effect of charge on the solute molecule on the calculated results is clear. Comparing the energies of the $H_2AsO_4^-$ and $HAsO_4^{2-}$ reactions shows an increase from –140 to –197 kJ mol^{-1} in favourability. Thus, using the appropriately charged species for comparison with experiment is critical in determining the most likely reactions. Of course, in a real system, as pH increases to favour $HAsO_4^{2-}$ over $H_2AsO_4^-$, the likelihood of interacting with positively charged surface sites such as $Fe_2(OH)_5(OH_2)_5^+$ also decreases.

A comparison of the model ΔG_{ads} of carbonate, arsenate and phosphate shows that ΔG_{ads} of arsenate > phosphate > carbonate. This result is consistent with the observation of Radu *et al*. (2005), who found that greater aqueous carbonate concentrations did not significantly displace adsorbed arsenate and that arsenate adsorbs more strongly than phosphate (Radu *et al*., 2005). We note that the calculated phosphate ΔG_{ads} is not thermodynamically favourable when the diprotonated, bidentate species $Fe_2(OH)_4(OH_2)_4H_2PO_4^+{\cdot}(H_2O)_4$ is the product. This is consistent with our previous calculations that showed the singly protonated, monodentate species as the stable surface complex near circumneutral pH based on comparison to IR frequencies and calculated adsorption energies (Kwon & Kubicki, 2004). The predicted thermodynamic favourability of sulphate adsorption was comparable with phosphate, and hence may compete effectively with similar adsorption sites. Experimental testing of this prediction would be useful in evaluating our computational approach.

Conclusions

Computational chemistry is a useful tool for studying surface reactions when used in combination with a variety of experimental techniques. Although system size and level of theory can limit the accuracy of these model calculations, results can be determined reliably enough to distinguish among various hypothesized structures. A good strategy is to use the flexibility of the MO/DFT calculations to predict a variety of experimentally observable properties, such as interatomic distances, vibrational frequencies and reaction free energies. Discovering one model that fits all the data best provides confidence in the molecular model derived from this effort. Interaction between experimentalists and modellers creates a feedback that improves the thought process from both aspects of a given research project. Recently, there has been a growing number of studies involving experimental IR work in conjunction with MO/DFT computations. However, systematic studies are required to answer fundamental questions with respect to surface complexation, for example:

1 How do vibrational frequencies change from solution to mineral surface complexes (e.g. new frequency emergence or shifting, etc.)?

2 How do chemical bonds between anions and mineral surface Fe atoms affect the system energy and oxyanion geometries?

3 Can we generalize the complex trends in observed vibrational frequencies and bonding geometries?

Increasing computational speed will continue to make it easier to produce high-quality computations on realistic systems in the future.

Acknowledgements

This research was funded by the NSF grant CHE-0221934 'Stony Brook-BNL collaboration to establish a Center for Environmental Molecular Sciences (CEMS)'. Computation was supported in part by the Materials Simulation Center, a Penn-State MRSEC and MRI facility, and the Center for Environmental Kinetics Analysis (CEKA), a NSF/DOE Environmental Molecular Sciences Institute.

References

Appelo, C.A.J., Van der Weiden, M.J.J., Tournassat, C. & Charlet, L. 2002. Surface complexation of ferrous iron and carbonate on ferrihydrite and the mobilization of arsenic. *Environmental Science and Technology*, **36,** 3096–3103.

Arai, Y., Elzinga, E.J. & Sparks, D.L. 2001. X-ray absorption spectroscopic investigation of arsenite and arsenate adsorption at the aluminum oxide–water interface. *Journal of Colloid and Interface Science*, **235,** 80–88.

Arai, Y. & Sparks, D.L. 2001. ATR-FTIR spectroscopic investigation on phosphate adsorption mechanisms at the ferrihydrite–water interface. *Journal of Colloid and Interface Science*, **241,** 317–326.

Arai, Y., Sparks, D.L. & Davis, J.A. 2004. Effects of dissolved carbonate on arsenate adsorption and surface speciation at the haematite–water interface. *Environmental Science and Technology*, **38,** 817–824.

Bargar, J.R., Kubicki, J.D., Reitmeyer, R. & Davis, J.A. 2005. ATR-FTIR spectroscopic characterization of coexisting carbonate surface complexes on haematite. *Geochimica et Cosmochimica Acta*, **69,** 1527–1542.

Becke, A.D. 1993. Density-functional thermochemistry. 3. The role of exact exchange. *Journal of Chemical Physics*, **98,** 5648–5652.

Becker, U., Rosso, K.M. & Hochella, M.F. 2001. The proximity effect on semiconducting mineral surfaces: a new aspect of mineral surface reactivity and surface complexation theory? *Geochimica et Cosmochimica Acta*, **65,** 2641–2649.

Brown, G.E., Henrich, V.E., Casey, W.H., Clark, D.L., Eggleston, C., Felmy, A. *et al*. 1999. Metal oxide surfaces and their

interactions with aqueous solutions and microbial organisms. *Chemical Reviews*, **99,** 77–174.

Cancès, E., Mennucci, B. & Tomasi, J. 1997. A new integral equation formalism for the polarizable continuum model: theoretical background and applications to isotropic and anisotropic dielectrics. *Journal of Chemical Physics*, **107,** 3032–3041.

Cossi, M., Scalmani, G., Rega, N. & Barone, V. 2002. New developments in the polarizable continuum model for quantum mechanical and classical calculations on molecules in solution. *Journal of Chemical Physics*, **117,** 43–54.

Dixit, S. & Hering, J.C. 2003. Comparison of arsenic (V) and arsenic (III) sorption onto iron oxide minerals: implications for arsenic mobility. *Environmental Science and Technology*, **37,** 4182–4189.

Farquhar, M.L., Charnock, J.M., Livens, F.R. & Vaughan, D.J. 2002. Mechanisms of arsenic uptake from aqueous solution by interaction with goethite, lepidocrocite, mackinawite, and pyrite: an X-ray absorption spectroscopy study. *Environmental Science and Technology*, **36,** 1757–1762.

Faure, G. 1998. *Principles and Applications of Geochemistry*. Prentice Hall, Upper Saddle River, NJ.

Felipe, M.A., Xiao, Y.T. & Kubicki, J.D. 2001. Molecular orbital modelling and transition state theory in geochemistry. In: Reviews in Mineralogy and Geochemistry, 42 (eds R.T. Cygan & J.D. Kubicki), pp. 485–531. Mineralogical Society of America, Chantilly, VA.

Fendorf, S., Eick, M.J., Grossl, P. & Sparks, D.L. 1997. Arsenate and chromate retention mechanisms on goethite.1. Surface structure. *Environmental Science and Technology*, **31,** 315–320.

Fitts, J.P., Machesky, M.L., Wesolowski, D.J., Shang, X., Kubicki, J.D., Flynn, G.W. *et al*. 2005. Second-harmonic generation and theoretical studies of protonation at the water/α-TiO_2 (110) interface. *Chemical Physics Letters*, **411,** 399–403.

Foresman, J.B. & Frisch, A. 1996. *Exploring Chemistry with Electronic Structure Methods*. Gaussian Inc, Pittsburgh, PA.

Frisch, M.J., Trucks, G.W., Schlegel, H.B., Scuseria, G.E., Robb, M.A., Cheeseman, J.R. *et al*. 2003. *Gaussian 03 (Revision C.01)*. Gaussian, Inc, Pittsburgh, PA.

Goldberg, S. & Johnston, C.T. 2001. Mechanisms of arsenic adsorption on amorphous oxides evaluated using macroscopic measurements, vibrational spectroscopy, and surface complexation modelling. *Journal of Colloid and Interface Science*, **234,** 204–216.

Hering, J.G., Chen, P.-Y., Wilkie, J.A. & Elimelech, M. 1997. Arsenic removal from drinking water during coagulation. *Journal of Environmental Engineering*, **123,** 800–807.

Hug, S.J. 1997. In situ Fourier transform infrared measurements of sulphate adsorption on haematite in aqueous solutions. *Journal of Colloid and Interface Science*, **188,** 415–422.

Keith, T.A. & Frisch, M.J. 1994. Inclusion of explicit solvent molecules in a self-consistent reaction field model of solvation. In: *Modeling the Hydrogen Bond*. (ed. D.A. Smith), pp. 22–35. American Chemical Society Symposium Series, 569. American Chemical Society, Washington DC.

Krishnan, R., Binkley, J.S., Seeger, R. & Pople, J.A. 1980. Self-consistent molecular-orbital methods. 20. Basis set for correlated wave-functions. *Journal of Chemical Physics*, **72,** 650–654.

Kubicki, J.D. 2005. Comparison of As (III) and As (V) complexation onto Al and Fe-hydroxides. In: *Advances in Arsenic Research: Integration of Experimental and Observational Studies and Implications for Mitigation* (eds P. O'Day, D. Vlassopoulos & L. Benning), pp. 104–117. ACS Symposium Series, 915. American Chemical Society, Washington DC.

Kubicki, J.D. & Apitz, S.E. 1998. Molecular cluster models of aluminum oxide and aluminum hydroxide surfaces. *American Mineralogist*, **83,** 1054–1066.

Kubicki, J.D., Itoh, M.J., Schroeter, L.M. & Apitz, S.E. 1997. Bonding mechanisms of salicylic acid adsorbed onto illite clay: an ATR-FTIR and molecular orbital study. *Environmental Science and Technology*, **31,** 1151–1156.

Kubicki, J.D., Sykes, D. & Rossman, G.R. 1993. Calculated trends of OH infrared stretching vibrations with composition and structure in aluminosilicate molecules. *Physics and Chemistry of Minerals*, **20,** 425–432.

Kwon, K.D. & Kubicki, J.D. 2004. Molecular orbital theory study on surface complex structures of phosphates to iron hydroxides: calculation of vibrational frequencies and adsorption energies. *Langmuir*, **20,** 9249–9254.

Lee, C.T., Yang, W.T. & Parr, R.G. 1988. Development of the Colle-Salvetti correlation-energy formula into a functional of the electron-density. *Physical Review B*, **37,** 785–789.

Manning, B.A., Fendorf, S.E. & Goldberg, S. 1998. Surface structures and stability of arsenic (III) on goethite: spectroscopic evidence for inner-sphere complexes. *Environmental Science and Technology*, **32,** 2383–2388.

McLean, A.D. & Chandler, G.S. 1980. Contracted gaussian-basis sets for molecular calculations. 1. 2nd row atoms, Z = 11–18. *Journal of Chemical Physics*, **72,** 5639–5648.

Myneni, S.C.B., Traina, S.J., Waychunas, G.A. & Logan, T.J. 1998. Experimental and theoretical vibrational spectroscopic evaluation of arsenate coordination in aqueous solutions, solids, and at mineral water interfaces. *Geochimica et Cosmochimica Acta*, **62,** 3285–3300.

Omoike, A., Chorover, J., Kwon, K.D. & Kubicki, J.D. 2004. Adhesion of bacterial exopolymers to alpha-FeOOH: inner-sphere complexation of phosphodiester groups. *Langmuir*, **20,** 11108–11114.

Overend, J. 1982. The experimental determination of gas-phase infrared intensities. In: *Vibrational Intensities in Infrared and Raman Spectroscopy* (eds W.B. Person & G. Zerbi), pp. 15–22. Elsevier, New York.

Parks, G.A. 1965. The isoelectric points of solid oxides, solid hydroxides, and aqueous hydroxo complex systems. *Chemical Reviews*, **65,** 177–198.

Paul, K.W., Borda, M.J., Kubicki, J.D. & Sparks, D.L. 2005. The effect of dehydration on sulphate coordination and speciation at the Fe-(hydr) oxide–water interface: a molecular orbital/density functional theory and Fourier transform infrared spectroscopic investigation. *Langmuir*, **21,** 11071–11078.

Paul, K.W., Kubicki, J.D. & Sparks, D.L. 2007. Sulphate adsorption at the Fe-(hydr) oxide–H_2O interface: Comparison of MO/DFT cluster and periodic DFT models. *European Journal of Soil Science*, **58,** doi: 10.1111/j.1365-2389.2007.00936.x.

Peng, C.Y., Ayala, P.Y., Schlegel, H.B. & Frisch, M.J. 1996. Using redundant internal coordinates to optimize equilibrium geometries and transition states. *Journal of Computational Chemistry*, **17,** 49–56.

Persson, P., Nilsson, N. & Sjoberg, S. 1996. Structure and bonding of orthophosphate ions at the iron oxide aqueous interface. *Journal of Colloid and Interface Science*, **177,** 263–275.

Petersson, G.A., Bennett, A., Tensfeldt, T.G., Al Laham, M.A., Shirley, W.A. & Mantzaris, J. 1988. A complete basis set model

chemistry. 1. The total energies of closed-shell atoms and hydrides of the 1st-row elements. *Journal of Chemical Physics*, **83,** 2193–2218.

Radu, T., Subacz, J.L., Phillippi, J.M. & Barnett, M.O. 2005. Effects of dissolved carbonate on arsenic adsorption and mobility. *Environmental Science and Technology*, **39,** 7875–7882.

Rosso, K.M., Becker, U. & Hochella, M.F. 1999. Atomically resolved electronic structure of pyrite {100} surfaces: an experimental and theoretical investigation with implications for reactivity. *American Mineralogist*, **84,** 1535–1548.

Schaftenaar, G. & Noordik, J.H. 2000. Molden: a pre- and post-processing program for molecular and electronic structures. *Journal of Computationally Aided Molecular Design*, **14,** 123–134.

Scott, A.P. & Radom, L. 1996. Harmonic vibrational frequencies: an evaluation of Hartree-Fock, Møller-Plesset, quadratic configuration interaction, density functional theory, and semiempirical scale factors. *Journal of Physical Chemistry*, **100,** 16502–16513.

Sherman, D.M. & Randall, S.R. 2003. Surface complexation of arsenic (V) to iron (III) (hydr) oxides: structural mechanism from ab initio molecular geometries and EXAFS spectroscopy. *Geochimica et Cosmochimica Acta*, **67,** 4223–4230.

Su, C.M. & Suarez, D.L. 1997. In situ infrared speciation of absorbed carbonate on aluminum and iron oxide. *Clays and Clay Minerals*, **45,** 814–825.

Usher, C.R., Paul, K.W., Narayansamy, J., Kubicki, J.D., Sparks, D.L., Schoonen, M.A.A. *et al.* 2005. Mechanistic aspects of pyrite oxidation in an oxidizing gaseous environment: an in situ HATR-IR isotope study. *Environmental Science and Technology*, **39,** 7576–7584.

Waychunas, G.A., June, Y.-S., Eng, P., Ghose, S.K. & Trainor, T.P. 2006. Anion sorption topology on haematite surfaces: comparison of arsenate and silicate. *Abstracts of Papers of the American Chemical Society*, **231,** 24–GEOC.

Waychunas, G.A., Rea, B.A., Fuller, C.C. & Davis, J.A. 1993. Surface chemistry of ferrihydrite: Part 1. EXAFS studies of the geometry of coprecipitated and adsorbed arsenate. *Geochimica et Cosmochimica Acta*, **57,** 2251–2269.

Wijnja, H. & Schulthess, C.P. 2001. Carbonate adsorption mechanism on goethite studied with ATR-FTIR, DRIFT, and proton coadsorption measurements. *Soil Science Society of America Journal*, **65,** 324–330.

Wijnja, H. & Schulthess, C.P. 2002. Effect of carbonate on the adsorption of selenate and sulphate on goethite. *Soil Science Society of America Journal*, **66,** 1190–1197.

Wong, M.W. 1996. Vibrational frequency prediction using density functional theory. *Chemical Physics Letters*, **256,** 391–399.

Yamaguchi, Y., Frisch, M., Gaw, J., Schaefer, H.F. III & Binkley, J.S. 1986. Analytic evaluation and basis set dependence of intensities of infrared spectra. *Journal of Chemical Physics*, **84,** 2262–2278.

Zhang, Z., Fenter, P., Cheng, L., Sturchio, N.C., Bedzyk, M.J., Předota, M. *et al.* 2004. Ion adsorption at the rutile–water interface: linking molecular and macroscopic properties. *Langmuir*, **20,** 4954–4969.